Clays and Clay Minerals, Vol. 42, No. 6, 717–723, 1994.

ACID HYDROLYSIS OF OCTAHEDRAL Mg^{2+} SITES IN 2:1 LAYERED SILICATES: AN ASSESSMENT OF EDGE ATTACK AND GALLERY ACCESS MECHANISMS

HEMAMALI KAVIRATNA AND THOMAS J. PINNAVAIA

Department of Chemistry and Center for Fundamental Materials Research
Michigan State University, East Lansing, Michigan 48824

Abstract—The acid hydrolysis products of trioctahedral fluorohectorite and phlogopite have been investigated by XRD, MAS NMR spectroscopy and nitrogen BET surface area analysis in an effort to assess the relative importance of edge attack and gallery access mechanisms. A dramatic loss of X-ray crystallinity and the formation of Q^3 and Q^4 SiO_4 sites accompanied the depletion of Mg^{2+} from the octahedral sheet of both 2:1 layered structures. Depending on the extent of hydrolysis, the products derived from fluorohectorite exhibited surface areas up to 208 m^2/g, whereas phlogopite hydrolysis products gave values <20 m^2/g. The dramatic differences in surface areas were not related to differences in hydrolysis mechanisms. ^{19}F MAS NMR studies indicated that the hydrolysis of fluorohectorite occurred primarily by an edge attack mechanism equivalent to the hydrolysis pathway for phlogopite. A gallery access mechanism contributed to the hydrolysis of fluorohectorite only at the later stages of octahedral Mg^{2+} depletion. Solvation effects appeared to be important in determining the surface areas of the reaction products derived from the swelling (fluorohectorite) and non-swelling (phlogopite) precursors.

Key Words—Acid hydrolysis, Fluorohectorite, Mechanism, Phlogopite.

INTRODUCTION

The selective depletion of octahedral cations from the structures of 1:1 and 2:1 layered aluminosilicates by acid hydrolysis has been studied as a means of obtaining soluble Al^{3+} for electrochemical conversion to aluminum metal (Johnson *et al* 1964). More recently, acid hydrolysis reactions of many different clay minerals have been investigated as routes to high surface area silicates with properties well suited as adsorbents, catalysts, and composite filling materials (Gonzalez *et al* 1982, 1984; Dandy and Nadiye-Tabbiruka 1982; Corma *et al* 1984; Corma and Perez-Pariente 1987; Acosta *et al* 1984). Octahedral cations such as Al^{3+}, Fe^{3+}, Fe^{2+}, and Mg^{2+} can be depleted by treating the clay minerals with acids at elevated temperatures (Johnson *et al* 1964; Corma *et al* 1987) with the rates of depletion generally following the order $Mg^{2+} > Fe^{2+}$, $Fe^{3+} > Al^{3+}$ (Corma *et al* 1987; Luce *et al* 1972; Rice and Strong 1974). There has been considerable interest in the acid hydrolysis of 2:1 clay structures, especially palygorskite (Corma *et al* 1987, 1990; Gonzalez *et al* 1989), sepiolite (Corma *et al* 1986; Rodriguez-Reinoso *et al* 1981), montmorillonite (Mendioroz *et al* 1987; Rhodes and Brown 1992; Srasra *et al* 1989), and vermiculite (Suquet *et al* 1991). BET surface areas as high as 500 m^2/g have been reported for the amorphous silicates derived from some of these minerals.

The general mechanism for the depletion of metal ions from the octahedral sheet of 2:1 layered structures involves proton attack at the edges of the layers. Evidence for edge attack is provided in part by the dependence of hydrolysis rates on the particle size of a non-swelling clay (Cetisli and Gedikbey 1990). However, the possibility of hydrolysis occurring by proton attack through the ditrigonal cavities of the basal surfaces also has been recognized in the case of swelling smectitic clays, wherein protons can easily occupy the gallery surfaces by ion exchange (Rice and Strong 1974). Figure 1 schematically illustrates these two available pathways for Mg^{2+} hydrolysis from trioctahedral 2:1 structures.

The hydrolysis of swelling and non-swelling trioctahedral 2:1 clays can result in hydrolysis products with dramatically divergent physical properties, as will be shown in the present work. The acidic hydrolysis of fluorohectorite produces products with BET surface areas up to 208 m^2/g, whereas the equivalent hydrolytic reactions of phlogopite yield products with surface areas no larger than 20 m^2/g. Such differences in properties might be linked to differences in hydrolysis mechanism. The objective of the present study was to evaluate the possible role of a "gallery access" or "edge attack" mechanism in the hydrolysis of these two typical trioctahedral smectites.

EXPERIMENTAL METHODS

Starting materials

A synthetic fluorohectorite with an anhydrous unit cell formula of $Li^+_{1.2}$ $[Mg_{4.8}Li_{1.2}][Si_8]O_{20}F_4$ was obtained from Corning, Inc. This smectite was selected for study because it exhibits ^{19}F NMR lines that are sensitive to hydrolytic displacement reactions of the octahedral sheet (Butruille *et al* 1993). Owing to the relatively large platelet size (~ 0.2 μm), the BET surface

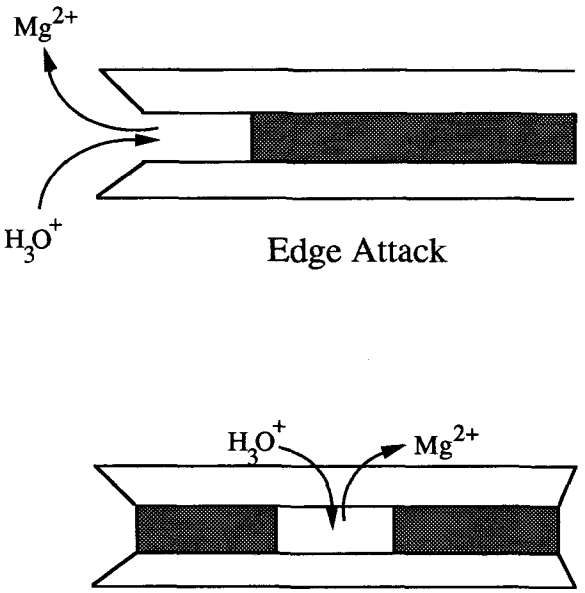

Figure 1. Schematic illustration of the depletion of octahedral Mg^{2+} from 2:1 layered silicates by proton edge attack and gallery access mechanisms.

area of the pristine clay after degassing under vacuum at 150°C was only 3 m^2/g. Phlogopite from North Burgess, Ontario with 2–6 m^2/g surface area was chosen as a representative non-swelling 2:1 structure and was ground to <100 mesh particles. Magnesium analysis was in agreement with an idealized unit cell formula of $K_2[Mg_6][Al_2Si_6]O_{20}(OH)_4$.

Hydrolysis reactions

Acid hydrolysis reactions of fluorohectorite were carried out in 0.5 M hydrochloric acid at 60°C. A higher hydrochloric acid concentration (5.0 M) and reaction temperature (105°C) was used to speed up the hydrolysis rate of the larger particle sized phlogopite. All reactions were carried out in a glass reaction flask equipped with a reflux condenser to prevent the loss of water. Five times the stoichiometric amounts of acids were used to achieve the hydrolysis of the octahedral cations of both silicates. The hydrolyzed residues were washed free of Cl^- with distilled deionized water and air dried. The solid products and the filtrates were analyzed for Mg^{2+} using a Direct Current Plasma (DCP) analyzer.

Physical measurements

XRD patterns were recorded on a Rigaku rotaflex diffractometer equipped with DMAXB software and Ni-filtered Cu K_α X-ray radiation. The ^{19}F and ^{29}Si MAS NMR experiments were performed on a Varian

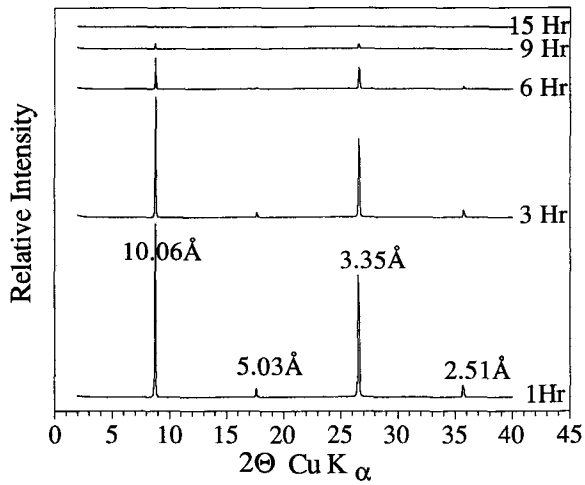

Figure 2. X-ray powder diffraction patterns showing the time-dependent loss in crystallinity of phlogopite upon acid hydrolysis in 5.0 M HCl at 105°C.

400 VXR solid state NMR spectrometer. A Bruker multinuclear MAS probe equipped with zirconia rotors was used for ^{29}Si MAS NMR measurements. The ^{29}Si spin-lattice relaxation times (T_1) were determined by the inversion recovery method. A total of 12 scans were accumulated for each sample. The spinning rate was 4.2 kHz. Delay time was 600 s, which was 5 times as large as the longest T_1 of ^{29}Si MAS NMR signals. Cross polarization experiments were carried out with delay times of 10 sec and contact times of 1000 ms. ^{19}F MAS NMR spectra were obtained using a Doty probe with 350 s delay time. The ^{19}F chemical shifts are relative to hexafluorobenzene. Adsorption measurements were carried out on an Omnisorb 360CX Coulter instrument using nitrogen as the adsorbate at 77 K. Surface areas were calculated according to the BET method.

RESULTS AND DISCUSSION

Phlogopite hydrolysis

We consider first the hydrolysis of phlogopite in 5.0 M HCl at a reaction temperature of 105°C. Under these conditions the mineral undergoes structural destruction due to dissolution of the octahedral cations, but there is no evidence based on X-ray diffraction for intragallery ion exchange. As can be seen from the powder patterns in Figure 2, the dominant 001 reflection characteristic of the pristine mineral (d_{001} = 1.00 nm) simply decreases with increasing reaction time without undergoing line broadening. Thus, the rate of ion exchange is much smaller than the rate of layer hydrolysis. That is, the gallery access pathway is precluded, and the depletion of Mg^{2+} from the octahedral sheet can only occur by proton attack at layer edge sites.

Table 1 summarizes the depletion of octahedral Mg^{2+}

Table 1. Mg^{2+} depletion and BET surface areas for acid hydrolyzed phlogopites.

Reaction time (hours)	Mg^{2+} depleted (%)	Surface area (m^2/g)
0	0	3
1	53	18
2	66	
3	69	
4	87	16
6	87	14
7	88	16
9	91	
11	94	
13	98	14
15	>99	
72	~100	11

Reactions were carried out at 105°C in 5.0 M HCl at a $H^+ : Mg^{2+}$ molar ratio of 5:1.

and the BET surface areas of selected hydrolysis products as a function of reaction time. The surface area increases from 3 m^2/g for the unhydrolyzed sample to an optimum value of 18 m^2/g at 53% Mg^{2+} depletion. Increasing the Mg^{2+} depletion to 100% lowers the surface area to 11 m^2/g. Assuming that all of the residual magnesium at the 53% depletion level is associated with the unhydrolyzed phlogopite phase, we estimate the *maximum* obtainable surface area for a hydrolyzed product to be 31 m^2/g. We note that Harkonen and Keiski (1984) have reported a surface area of 620 m^2/g for acid treated phlogopite obtained as a by-product in the processing of appatite. Our attempt to reproduce the hydrolysis chemistry of Harkonen and Keiski with the phlogopite used in this study gave a surface area of only 32 m^2/g.

Pristine phlogopite normally exhibits three ^{29}Si MAS NMR lines in accord with Q^3 SiO_4 sites linked to 0 AlO_4, 1 AlO_4, or 2 AlO_4 tetrahedra (Sanz and Serratosa 1984). Owing to the presence of paramagnetic impurities (iron), the sample used in the present study exhibits three broad overlapping resonances centered near −86 ppm. As shown by the ^{29}Si MAS NMR spectrum in Figure 3A, the hydrolysis product at 53% Mg^{2+} depletion gives rise to overlapping Q^3 and Q^4 resonances at −103 and about −112 ppm, respectively. Direct evidence for the presence of Q^3 silicon environments is provided by the ^1H-^{29}Si cross polarized spectrum in Figure 3B. The upfield shift in the Q^3 resonance from −86 to −103 ppm suggests that some aluminum is leached from the tetrahedral sheets upon hydrolysis. Also, the Q^3 resonance of the residual phlogopite overlaps the Q^3 line for the amorphous aluminosilicate formed by hydrolysis. At 100% Mg^{2+} depletion the hydrolyzed product exhibits a broad ^{29}Si resonance centered at 112 ppm in agreement with a highly cross linked amorphous aluminosilicate containing primarily Q^4 Si sites. A single broad ^{27}Al resonance indicative

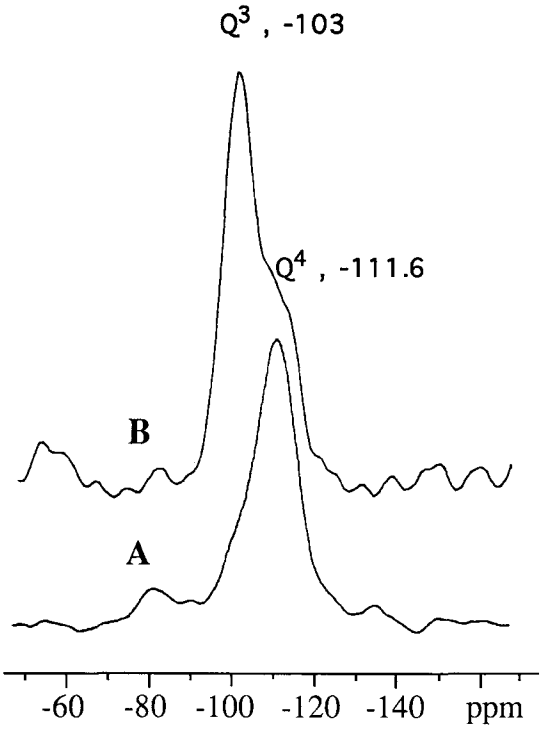

Figure 3. (A) ^{29}Si MAS NMR spectrum of acid hydrolyzed phlogopite at 53% Mg^{2+} depletion. (B) Spectrum repeated under ^1H-^{29}Si cross polarization.

of tetrahedral aluminum is observed at ~70 ppm for the magnesium-free hydrolysis product.

Fluorohectorite hydrolysis

Owing in part to a greatly reduced particle size fluorohectorite is much more reactive toward acid hydrolysis than phlogopite. Octahedral Mg^{2+} depletion rates comparable to those reported above for phlogopite can be achieved using a much lower acid concentration (0.5 M HCl) and reaction temperature (60°C). Similar reactivities have been observed for the acid hydrolysis of the inverted 2:1 layered silicates sepiolite (Rodriguez-Reinoso *et al* 1981; Corma *et al* 1986) and palygorskite (Gonzalez *et al* 1989).

Figure 4 shows selected X-ray powder diffraction patterns for acid hydrolyzed fluorohectorite samples. It is clear from the disappearance of the 001 reflection that no long range crystallinity is retained after a 2 hour reaction time in the presence of a five-fold excess of 0.5 M HCl at 60°C. Table 2 lists the Mg^{2+} depletion levels and BET surface areas for representative hydrolysis products of fluorohectorite. The surface areas increase substantially from 3 m^2/g for the parent clay to values of 111–208 m^2/g, depending on the extent of hydrolysis. It is noteworthy that the hydrolysis of fluorohectorite in 5.0 M rather than 0.5 M HCl does not reduce the surface area of the hydrolysis product to the

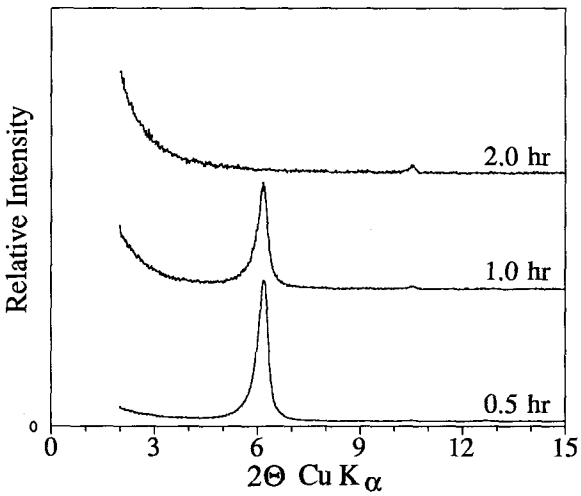

Figure 4. X-ray powder diffraction patterns of acid hydrolyzed fluorohectorites in a five-fold excess of 0.5 M HCl at 60°C.

low value obtained for hydrolyzed phlogopite. As can be seen from the last entry in Table 2, the surface area obtained after hydrolysis in 5.0 M HCl is still high, 151 m^2/gM HCl. Thus our results are in agreement with previous reports on the acid hydrolysis products of magnesium-rich palygorskite (Corma *et al* 1990; Gonzalez *et al* 1989), sepiolite (Rodriguez-Reinoso *et al* 1981), and vermiculite (Lopez-Gonzales *et al* 1959, Suquet *et al* 1991) insofar as the crystallinity of the 2:1 structure decreases with acid treatment, while the BET surface area increases.

Figure 5 shows the ^{29}Si MAS NMR spectra of acid hydrolyzed phlogopites at 36%, 62% and 83% levels of Mg^{2+} depletion. The line at −93.3 ppm is assigned to the Q^3 SiO_4 sites of the parent clay. The lines at −103 and −112 ppm, respectively, are assigned to Q^3 sites containing Si-OH linkages and to Q^4 sites in the amorphous reaction product. CP ^{29}Si MAS NMR spectroscopy confirmed the Q^3 assignment for the hydrolysis product. Thus, the amorphous hydrolysis products obtained from fluorohectorite and phlogopite have

Table 2. Mg^{2+} depletion and BET surface areas for acid hydrolyzed fluorohectorites.

Reaction time (hours)	Mg% depleted	Surface area (m^2/g)
0.0	0	3
0.5	36	111
1.0	62	201
2.0	83	208
1.0[1]	100	151

Reactions were carried out in 0.5 M HCl at 60°C and a molar H^+ : Mg^{2+} ratio of 5 : 1.

[1] This product was formed by reaction with 5.0 M HCl at 105°C.

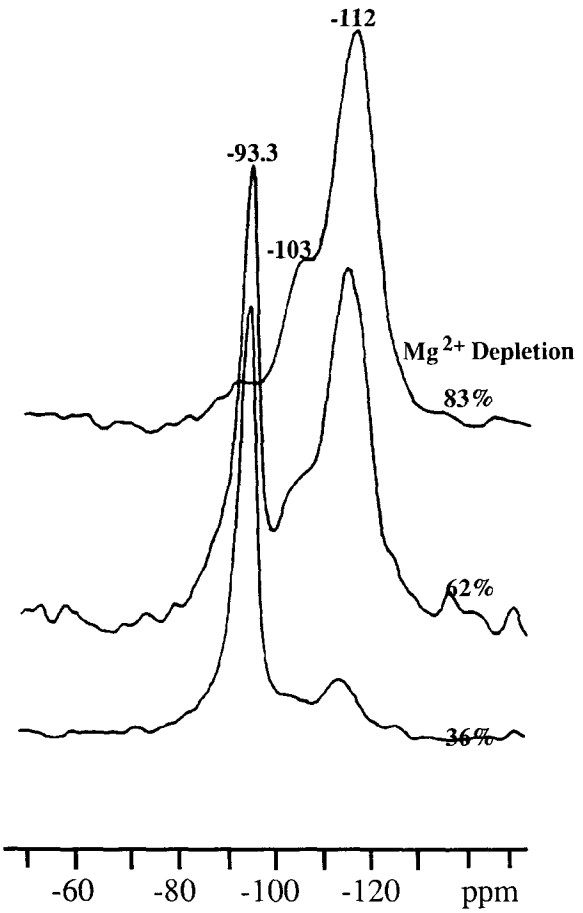

Figure 5. ^{29}Si MAS NMR spectra of acid hydrolyzed fluorohectorites with different levels of Mg^{2+} depletion.

similar Q^3 and Q^4 connectivities, but they differ dramatically in surface areas.

^{19}F MAS NMR spectroscopy provides further important insight into the structural consequences of fluorohectorite hydrolysis. Spectra for representative reaction products are shown in Figure 6. The presence of two resonances agrees with earlier studies of fluorinated 2:1 structures (Butruille *et al* 1993; Huve *et al* 1992). The upfield line at −16 ppm arises from fluorine atoms triply bridging a positively charged triad of edge-shared octahedra occupied by two Mg^{2+} ions and one Li^+ ion. The lower field resonance (−11 ppm) is assigned to fluorine atoms bridging a neutral triad of octahedra filled by three Mg^{2+} ions. In the pristine mineral the two lines are of nearly equal intensity, in accord with the unit composition $Li^+_{1.2}$ $[Mg_{4.8}Li_{1.2}][Si_8O_{20}]F_4$. Upon depletion of Mg^{2+} from the octahedral sheet the intensities of the two ^{19}F resonances decrease due to HF formation, but the relative intensities remain almost unchanged up to a Mg^{2+} depletion level of 62%. That is, fluorine and magnesium hydrolysis occur concomitantly, and the rates of Mg^{2+} de-

pletion from charged and neutral octahedral triads are similar. However, as the extent of Mg^{2+} hydrolysis nears the 80% level, the charged triads are preferentially hydrolyzed, as judged by the unequal intensities of the fluorine lines (Figure 6).

Mechanistic implications and significance

The above results demonstrate that the acidic hydrolysis of Mg^{2+} from the layers of non-swelling phlogopite and swelling fluorohectorite is accompanied in both cases by the loss of X-ray diffraction effects and by the formation of amorphous silicate reaction products containing Q^3 and Q^4 SiO_4 connectivities. Nevertheless, the reaction products differ greatly in total surface area. Depending on the extent of hydrolysis, BET surface areas up to 208 m^2/g are found for fluorohectorite reaction products, whereas values less than 20 m^2/g are observed for products derived from phlogopite. These differences cannot be attributed to differences in the acid concentrations used in the hydrolysis reactions. Low surface area products (<20 m^2/g) are formed from phlogopite upon reaction with 0.5 M HCl, and a high surface area (~ 150 m^2/g) is observed for magnesium-free silica formed by hydrolysis of fluorohectorite in 5.0 M HCl. These important differences in surface areas also can not be attributed to differences in reaction mechanism.

For the structural reasons already discussed, non-swelling phlogopite should hydrolyze primarily by an edge attack mechanism, whereas swelling fluorohectorite is potentially capable of undergoing hydrolysis by proton edge attack and/or gallery access mechanisms. However, the ^{19}F NMR results provide strong evidence for acid hydrolysis occurring primarily, though not exclusively, through an edge attack mechanism even in the case of the smectite clay. Butruille *et al* (1993) have shown in ^{19}F NMR studies of pillared fluorohectorites that the fluorine atoms bridging positively charged (Mg_2Li) triads in the octahedral sheet react with interlamellar water molecules through the dioctahedral cavities and become replaced by hydroxyl groups. In contrast, the fluorines bridging neutral (Mg_3) triads are stable toward displacement by hydroxyl groups. Thus, if Mg^{2+} hydrolysis occurred by a gallery access mechanism, we should expect the NMR lines for the two types of fluorine environments to decrease at different rates. Instead, we find that the two resonances decrease at essentially equal rates up to a Mg^{2+} depletion level of 62% (Figure 6). This result is in complete accord with proton attack at edge-site oxygen atoms of the octahedral sheet. At a Mg^{2+} depletion of 83%, the -16 ppm resonance for the fluorines bridging (Mg_2Li) triads decreases more rapidly than the -11 ppm line, signaling the strong effect of a gallery access mechanism. However, edge attack remains the primary Mg^{2+} depletion mechanism with at least two-thirds of the total structural Mg^{2+} being replaced by this pathway. It is not clear why the gallery access is manifested at the later stages of Mg^{2+} depletion. Perhaps the gallery access path is facilitated by the structural disorder and reduction in layer charge density caused by proton edge attack or the edge attack pathway becomes inhibited by the growing coating of silica at the edge sites.

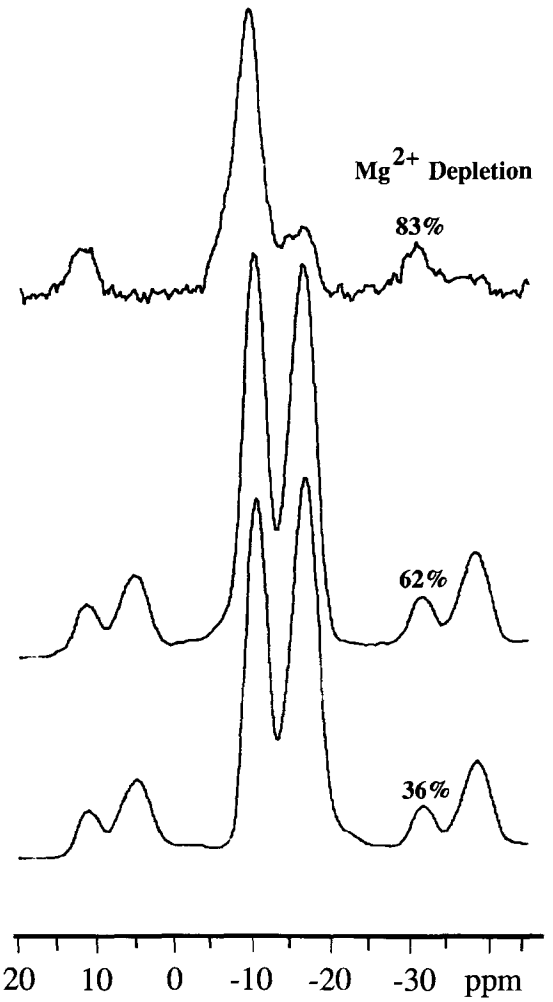

Figure 6. ^{19}F MAS NMR spectra of acid hydrolyzed fluorohectorites at different levels of Mg^{2+} depletion.

Since the hydrolysis reactions of fluorohectorite and phlogopite occur primarily through equivalent pathways, one is unable to attribute the differences in surface areas to structural effects caused by different reaction mechanisms. Instead, the swelling properties of the starting 2:1 structure most likely plays a central role in establishing the textural properties of the amorphous hydrolysis products. Hydration of the protonated fluorohectorite galleries separates the 2:1 layers during hydrolysis. We tentatively propose that the interlamellar water and protons serve in part to lower the bulk density of the silicate phase formed by the crosslinking of the residual tetrahedral sheets. As shown

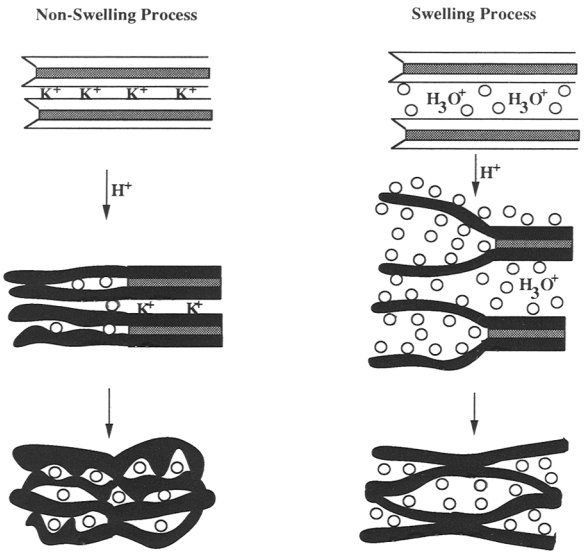

Figure 7. Schematic illustration of solvation effects on the textures of silicate products formed in the acid hydrolysis of swelling and non-swelling 2:1 structures. Open circles represent water molecules.

schematically in Figure 7, both surfaces of the evolving silicate layer can be efficiently solvated during the hydrolysis reaction, whereas the non-swelling phlogopite is relatively limited in its ability to mediate the texture of the hydrolysis product through solvation. Consequently, the surface areas of the phlogopite hydrolysis products are much lower than those formed from fluorohectorite.

Interlamellar water may also be important in mediating the edge attack hydrolysis of dioctahedral smectites. For instance, Rhodes and Brown (1992) recently reported a surface area of 320 m^2/g for an amorphous aluminosilicate formed by the acid hydrolysis of montmorillonite with 30% H_2SO_4 for 15 minutes. Similar considerations apply to the products formed by sepiolite and palygorskite hydrolysis. In these latter structures the 2:1 layers are periodically inverted, giving rise to channels that permit efficient hydration of the tetrahedral sheets and the formation of high surface area products.

CONCLUSIONS

An edge attack mechanism operates in the acid hydrolysis of fluorohectorite and phlogopite, yet substantial differences in surface areas are observed for the hydrolysis products of these trioctahedral 2:1 layered silicates. The swellable fluorohectorite typically affords hydrolysis products with surface areas ≥ 150 m^2/g, whereas the products obtained from non-swelling phlogopite exhibit areas ≤ 20 m^2/g. Differences in the extent of solvation of the silica formed at the hydrolytic interface may be responsible for the dramatic differences in the textural properties of the reaction products.

ACKNOWLEDGMENTS

The support of this research by the National Science Foundation through grants DMR-8903579 and CHE-9224102 is gratefully acknowledged.

REFERENCES

Acosta, J. L., C. M. Rocha, and M. C. Ojeda. 1984. The effect of several modified sepiolites on the transition temperatures and crystallinity of filled propylene. *D. Angew Makromol. Chemie.* **126**: 51–57.

Butruille, J-R, L. J. Michot, O. Barres, and T. J. Pinnavaia. 1993. Fluorine-mediated acidity of alumina-pillared fluorohectorite. *J. Catal.* **139**: 664–678.

Cetisli, H., and T. Gedikbey. 1990. Dissolution kinetics of sepiolite from Eskisehir (Turkey) in hydrochloric and nitric acids. *Clay Miner.* **25**: 207–215.

Corma, A., J. Perez-Pariente, V. Fornes, and A. Mifsud. 1984. Catalytic activity of modified silicates: I Dehydration of ethanol catalysed by acidic sepiolite. *Clays & Clay Miner.* **19**: 673–676.

Corma, A., A. Mifsud, and J. Perez. 1986. Etude cinetique de l'attaque acide de la sepiolite: Modifications des proprietes texturales. *Clay Miner.* **21**: 69–84.

Corma, A., and J. Perez-Pariente. 1987. Surface acidity and activity of a modified sepiolite. *Clay Miner.* **22**: 423–433.

Corma, A., A. Mifsud, and E. Sanz. 1987. Influence of the chemical composition and textural characteristics of palygorskite on the acid leaching of octahedral cations. *Clay Miner.* **22**: 225–232.

Corma, A., A. Mifsud, and E. Sanz. 1990. Kinetics of the acid leaching of palygoskite: Influence of the octahedral sheet composition. *Clay Miner.* **25**: 197–205.

Dandy, A. J., and M. S. Nadiye-Tabbiruka. 1982. Surface properties of sepiolite from Amboseli, Tanzania, and its catalytic activity for ethonol decomposition. *Clays & Clay Miner.* **30**: 347–352.

Gonzalez, L., R. L. Ibarra, and D. A. Rodriguez. 1982. Preparation of silica by acid dissolution of sepiolite and study of its reinforcing effect in elastomers. *D. Angew Makromol. Chemie.* **103**: 51–60.

Gonzalez, L., R. L. Ibarra, D. A. Rodriguez, J. S. Moya, and F. J. Valle. 1984. Fibrous silica gel obtained from sepiolite by HCl attack. *Clay Miner.* **19**: 93–98.

Gonzalez, F., C. Pesquera, I. Bennito, S. Mendioroz, and J. A. Parares. 1989. Structural and textural evolution of Al- and Mg-rich palygoskites, I. under acid treatment. *Appl. Clay Sci.* **4**: 373–388.

Harkonen, M. A., and R. L. Keiski. 1984. Porosity and surface area of acid leached phlogophite: The effect of leaching conditions and thermal treatment. *Colloids and Surfaces* **11**: 323–339.

Huve, L., L. Delomotte, P. Martin, R. Le Dred, J. Baron, and T. Saehr. 1992. 19F MAS-NMR study of structural fluorine in some natural and synthetic 2:1 layer silicates. *Clays & Clay Miner.* **40**: 186–191.

Johnson, D. W., F. A. Peters, and R. C. Kirby. 1964. Methods for producing alumina from clay. *Bur. Mines Rep. Invest. 27* **6431**: 1–25.

Luce, R. W., R. W. Bartlett, and G. A. Parks. 1972. Dissolution kinetics of magnesium silicates. *Geochimica et Cosmochimica Acta* **36**: 35–50.

Mendioroz, S., J. A. Pajares, I. Benito, C. Pesquera, F. Gonzalez, and C. Blanco. 1987. Texture evolution of montmorillonite under progressive acid treatment: Change from H3 to H2 type of hysteresis. *Langmuir* **3**: 676–681.

Rice, N. M., and L. W. Strong. 1974. The leaching of lateritic nickel ores in hydrochloric acid. *Canadian Metallurgical Quarterly* **b13**: 485–493.

Rhodes, C. N., and D. R. Brown. 1992. Structural characterisation and optimisation of acid-treated montmorillonite and high-porosity silica supports for $ZnCl_2$ alkylation catalysts. *J. Chem. Faraday Trans.* **88(15)**: 2269–2274.

Rodriguez-Reinoso, F., A. Ramirez-Sanz, J. De D. Lopez-Gonzalez, C. Valenzuela-Calahorro, and L. Zurita-Herrera. 1981. Activation of a sepiolite with dilute solutions of HNO_3 and subsequent heat treatment. *Clay Miner.* **16**: 315–385.

Sanz, J., and J. M. Serratosa. 1984. ^{29}Si and ^{27}Al high-resolution MAS-NMR spectra of phyllosilicates. *J. Am. Chem. Soc.* **106**: 4790–4793.

Srasra, E., F. Bergaya, H. Vandamme, and N. K. Ariauib. 1989. Surface properties of an activated bentonite-decoloration of Rape-seed oil. *Appl. Clay Sci.* **4**: 411–421.

Suquet, H., S. Chevalier, C. Marcilly, and D. Barthomeuf. 1991. Preparation of porous materials by chemical activation of the Llano vermiculite. *Clay Miner.* **26**: 49–60.

(Received 13 January 1994; accepted 7 June 1994; Ms. 2454)